Preparation of Monodisperse Carbonaceous Particles with Micro-, Meso-, and Macroporous Structures

KHALED M. DAER and YIANNIS A. LEVENDIS*

Department of Mechanical Engineering, Northeastern University, Boston, Massachusetts 02115

SYNOPSIS

Spherical, highly porous synthetic carbon particles have been prepared from formulations of either poly(furfuryl alcohol) or poly(vinyl acetate) mixed with a solvent and pore-forming agents. Production was carried out by atomizing these mixtures inside a thermal reactor and drying the resulting aerosol. The size of the collected polymeric particles was controlled by preadjusting the parameters of the atomization process. Fine-tuning of the process resulted in the generation of batches of monosized particles. Subsequent thermal degradation at 600°C resulted in porous chars with controlled pore-size distributions. Several distinct pore structures were superimposed using this technique with pore widths spanning the region from a few nanometers to a few tens of micrometers. Spherical and equal-sized macropores were also generated with a special technique described herein. All chars were produced in batches of spherical and monodisperse particles, with diameters in the range of 20–150 μm. BET surface areas were measured to vary from 1 m^2/g to over 150 m^2/g prior to any oxidative treatment. Porosities varied from 10 to 80%.

1. INTRODUCTION

Production of carbonaceous particles of controlled size and porosity can find applications in gas filtration, heterogeneous catalysis, studies on material properties, calibration of instruments, etc. Such particles can also be used as physical models in fundamental studies on char-pore diffusivity and capillary phenomena as well as on char oxidation and fragmentation. Typical industrial applications of microporous carbons range from catalyst supports to "activated" carbons, used as adsorbers and molecular sieves to remove impurities from gas and water streams. Manufacture of such carbons can be tailored to obtain a whole range of materials from those containing considerable microporosity to those embodying essentially no microporosity. Porous carbons usually exhibit polymodal pore-size distributions, with nominal diameters ranging from molecular dimensions to several hundred nanometers. This pore network creates a large internal surface area. However, depending on the sizes of the reactant and product molecules, a fraction of the surface area contained in smaller pores, and, thus, any catalyst contained therein, may be inaccessible for reaction. Hence, it is of technological interest to produce pure carbons with desired shape, size, porosity, and surface area as well as controlled pore-size distribution.

Microporous carbons have a very disordered atomic structure, as revealed by a variety of analytical techniques (TEM, SEM, XRD, SAXS, EXAFS, etc.) and various model structures have been proposed based on studies of polymer carbons,[1] carbon fibers,[2] carbonized coals,[3] and activated carbons.[4] Although the models differ in detail, the essential common feature is a twisted network of defective carbon layer planes, cross-linked by aliphatic bridging groups. The layer planes occur singly or in small stacks of two, three, or four with variable interlayer spacings in the range of 0.34–0.8 nm.[5] Empty spaces between these crystallites constitute the micropores,† which are usually slit-shaped.[6] It should be

* To whom correspondence should be addressed.

Journal of Applied Polymer Science, Vol. 45, 2061–2073 (1992)
 CCC 0021-8995/92/122061-13$04.00

† An accepted size classification of pores by their width, w, or diameter is the following[1]: macropores, $w > 50$ nm; mesopores, $2 < w < 50$ nm; and micropores, $w < 2$ nm.

noted here that the pore network of any given carbon may not be interconnected and available to reaction in its entirety because of pore constrictions. These constrictions may be due to volatile pyrolysis products or to the presence of functional groups attached to the edges of layer planes.[7]

Porous carbons have been obtained in prior art by thermal treatment (activation) of a suitable material, such as coal or wood charcoal, with the aid of oxidizing agents.[8] These oxidizing agents (O_2, CO_2, steam, etc.) gasify portions of the carbon matrix, leaving behind pores. Thus, the microporous structure of coals,[9-15] active carbons,[16-18] and polymer-based carbons[19-29] can be altered by thermal treatment (inert or oxidative) at temperatures of a few hundred degrees Celcius (<1000°C). Under such treatment, the pore walls are receding and the constrictions are removed, increasing the porosity. At higher temperatures, however, sintering may take place in which case the pore network collapses.[19] An exception here are the highly cross-linked carbons that resist sintering.[25-27] Therefore, by carefully activating selected carbonaceous precursors, the size of pores can be sufficiently controlled to generate carbons that exhibit specificity in rendering access to different liquid or gas molecules. Carbons with precisely controlled pore-size distribution, however, cannot be produced using this procedure, since during activation new pores are continuously forming or opening up while existing pores are constantly being enlarged.[30] In addition to the difficulty of controlling the pore-size distribution, this reacting away of the carbon weakens the final structure. Thus, many efforts have been undertaken to prepare synthetic carbons with tailored pore structure[21,22,26,29] without resorting to activation. Most of these studies were concerned with producing carbons in bulk, a process that is time-consuming.

In recent years, several methods have been proposed to produce porous synthetic carbons in powder form using various polymeric precursors like ethylene glycol dimethylacrylate,[30] vinylidene chloride,[30,31] acrylonitrile,[32] divinyl benzene,[33] saran,[34] and furfuryl alcohol (PFA).[27,35] Techniques employed include preparation of carbons from polymer colloids by emulsion or suspension polymerization,[30-32] nebulization of polymer solutions, reacting vapors to form liquid aerosol droplets,[33] and atomization of dissolved polymers.[26] Gangolli et al.[33] obtained spherical amorphous carbon particles, 3–5 μm in diameter, by thermal degradation of poly(divinyl benzene) powder, consisting of spheres, 8 μm in diameter, in an inert atmosphere at 500°C. The powder colloid was generated by an aerosol technique. The resulting carbon particles had large specific area that indicated a high degree of porosity. The external surface of the spheres, however, appeared fairly smooth.

Levendis and Flagan[26] developed an expedient method of producing batches of uniform-sized glassy carbon spheres, both solid and hollow, in the size range of a few to 200 μm. Production time was in the order of seconds to minutes. The particles were prepared by atomizing solutions of poly(furfuryl alcohol) in acetone mixed with liquid pore-forming agents or carbon black. After additional heat treatment and/or partial oxidation in the temperature range of 800–1600 K, they were able to vary the porosity (6–50%) and the surface area (2–800 m^2/g), as well as to generate controlled pore-size distributions that included both micro- and mesopores. These hard, carbonized, highly cross-linked spheres were subsequently used as model materials in combustion studies.[36,37]

The work described herein pertains to the production of porous carbon powders consisting of spherical and monodisperse carbonaceous particles of any predetermined size in the range of a few to 150 μm. The aerosol generation technique of Levendis and Flagan[26] was employed to produce these particles and explore new methods for pore formation in carbons. Two different polymer binders have been used this time: poly(furfuryl alcohol) (PFA) and poly(vinyl acetate) (PVAC) in which pore-forming agents have been added. Several solid particles were used in this study as pore-forming agents, with emphasis placed in devising techniques to create macropores. Furthermore, the effect of the structure of solid pore formers in creating mesopores has been investigated.

2. EXPERIMENTAL

2.1. Apparatus and Procedure

To produce spherical and monodisperse droplets from a polymeric fluid, an aerosol generator was constructed, based on a previous design.[26] This instrument superimposes acoustic oscillations from a piezoelectric transducer on a stream of liquid passing through a small orifice. At an optimum high-frequency range, these instabilities lead to the breakup of the liquid jet into uniformly sized (monodisperse) droplets.[38] The size of the droplets is controlled by the size of the orifice, the oscillator's frequency, and the liquid feed rate. Consequently, the size of the dried particle depends on all the above parameters

in addition to the degree of dilution of the polymer (mass fraction of solvent). For example, the production of carbon particles of sizes in the range of 45–100 μm involved the following process conditions: orifices in the diameter range of 75–100 μm, oscillation frequencies of 14–18 kHz, and a liquid-feed flow rate of 1.6 cc/min. A high-pressure syringe pump, Harvard Apparatus 909, was employed to feed

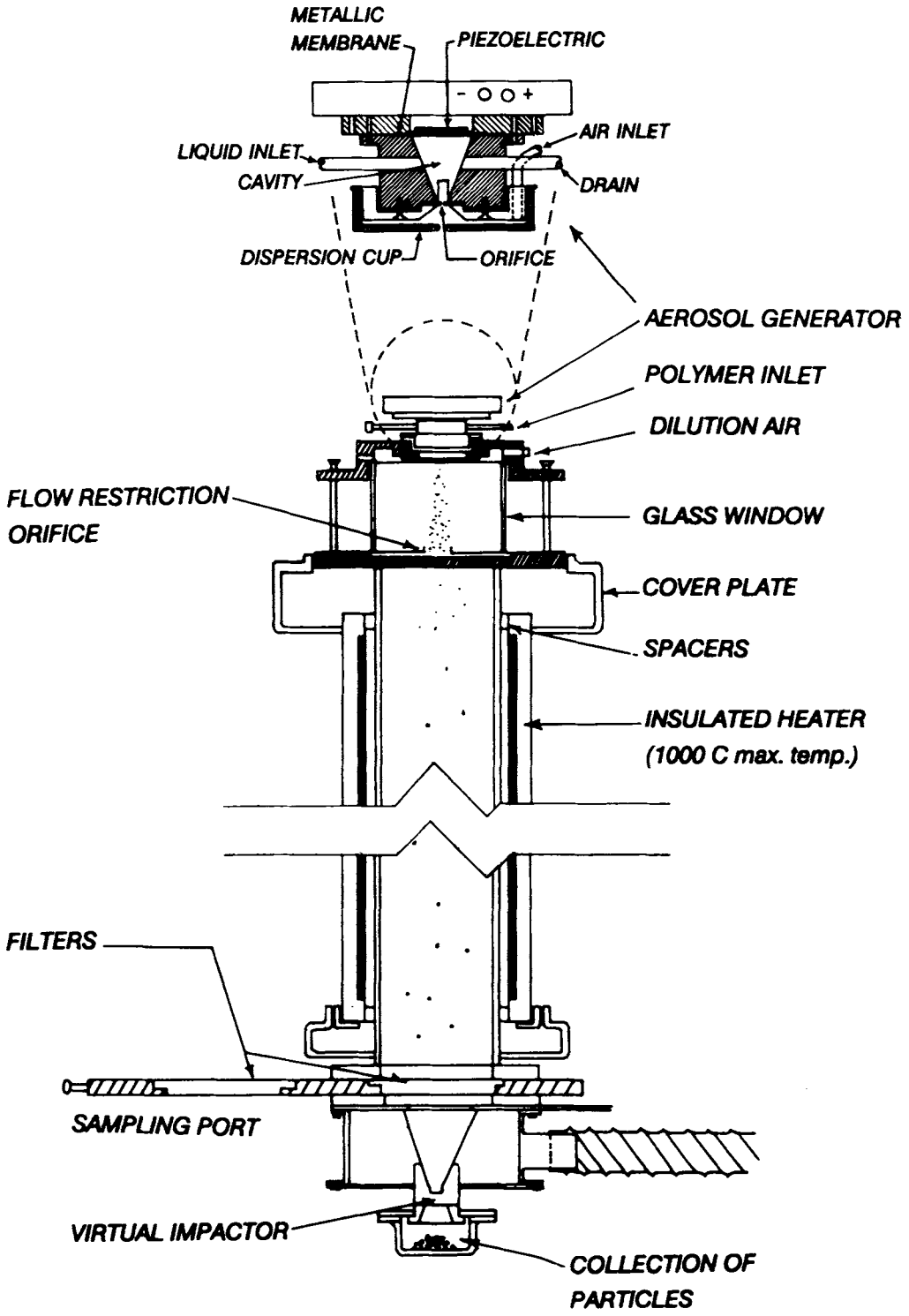

Figure 1 Schematic of the acoustically excited aerosol generator and the thermal reactor.

dissolved polymers, or monomer catalyst mixtures, to the aerosol generator via Becton Dickinson plastic syringes. A specially constructed, two-stage thermal reactor, heated by Thermoline heating elements (6800 W), was employed for drying and curing the aerosol droplets. The droplets were produced at the top of the reactor, where the aerosol generator was mounted (Fig. 1). This stainless-steel flow reactor is 1.5 m high, 0.1 m i.d., and externally heated to wall temperatures up to 1000 K. Provisions for collecting the solid particles on paper filters were incorporated at the bottom of the reactor, where a sampling port was installed.

2.2 Particle Generation and Characterization

There are four basic ingredients for preparing the porous carbonaceous particles, namely, a carbon-yielding binder, a pore-forming agent, and a consolidating agent or polymerization catalyst.[27] Two different polymeric materials (i) PFA and (ii) PVAC were chosen as binders for this investigation. The former produces a high yield of char (49.1%) that is extensively cross-linked and nongraphitizing.[3,19,26] The latter yields only 4.7 wt % of char residue that has been reported to be graphitizing.[39] Triton was used as a dispersing agent (2 wt %) in all solutions. The catalyst that was used for the polymerization of PFA was *para*-toluene sulfonic acid (PTSA). The procedure for preparing these chars was as follows[40]:

The furfuryl alcohol monomer (Aldrich) was polymerized at 60°C in the presence of PTSA for 20 min, and the resulting polymer was dissolved in acetone at mass fractions ranging from 10 to 30%. The PVAC in powder form (Aldrich) was dissolved in acetone at a mass fraction of 7%. Both solutions were sonicated for 20 min; the PFA–acetone solution was also centrifuged for 10 min to precipitate any polymer particles.

Solid pore-forming agents, like carbon black particles, biological spores, and polystyrene beads were subsequently mixed in the binder–acetone solutions to serve as pore-forming agents. Three different kinds of carbon black were used with PFA, in concentrations of 20% by weight of the polymer [Fig. 2(a–c)]; (i) carbon lamp black (Fisher), (ii) monarch 1300, and (iii) black pearls 120 (the latter two from Cabot). PVAC was mixed with carbon lamp black only (20 wt %). The spores were bacteria *Bacillus subtilus* and were cylindrical in shape with dimensions $\approx 0.5 \times 1$ μm [Fig. 3(a)]. Polystyrene spheres were produced in house using the same equipment and similar techniques.[41] However, to avoid dissolution of the polystyrene spheres in the

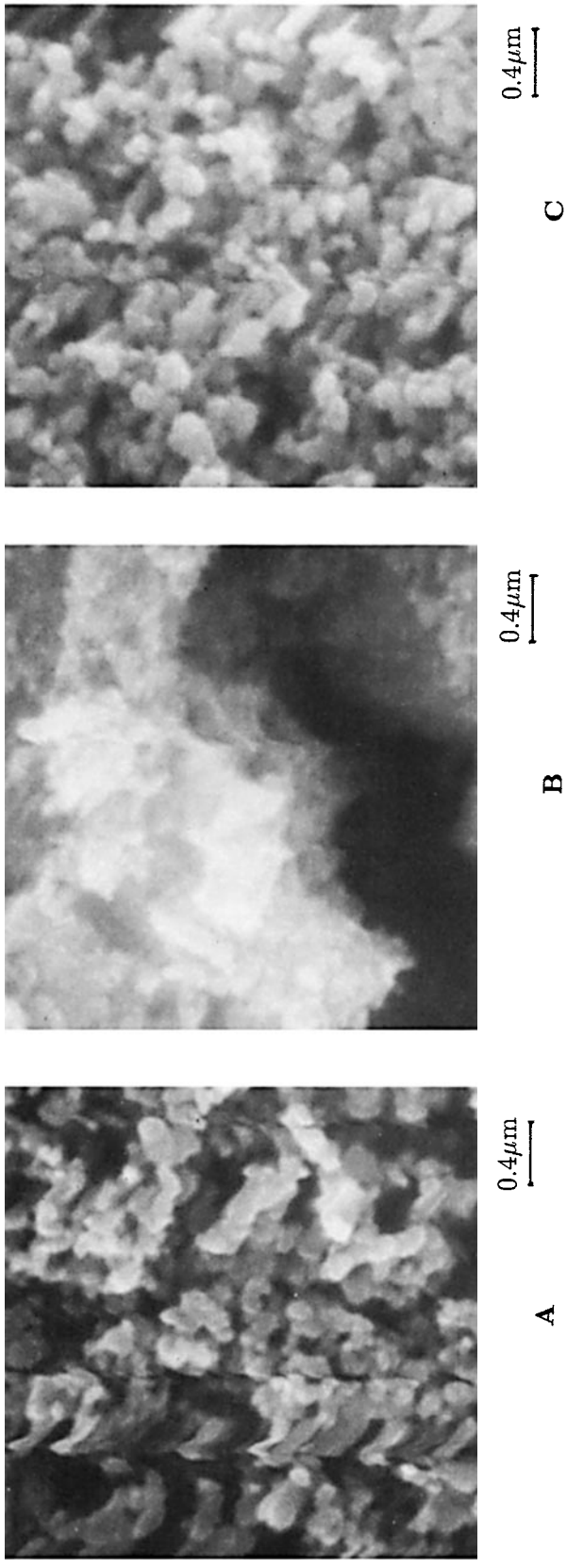

Figure 2 SEM photographs of the three types of CBs used as pore formers: (a) lamp black, (b) monarch black 1300, and (c) black pearls 120.

binder–acetone mixture, the polymer had to be extensively cross-linked. Production of cross-linked polystyrene particles was achieved by generating an aerosol of partially polymerized styrene monomer. The monomer was mixed with the polymerization catalyst benzoyl peroxide (2% by weight) and the cross-linking agent divinyl benzene (5% by weight) and was heated at 84°C in a nitrogen atmosphere for 16 min. Production was conducted by feeding this mixture, dissolved in toluene 90% by mass, to the generator. Atomization was achieved using a 20 μm orifice and an excitation frequency of $\approx$70 kHz and a liquid flow rate of 0.21 cm^3/s. The residence time in the reactor was in the order of 5–10 s. The temperature profile in the reactor was controlled to prevent flash-vaporization of the monomer. Thus, the top section of the reactor was set at a temperature of 240°C to provide for slow initial heat-up, and the bottom section was hotter (300°C) to allow for the polymerization reactions to proceed to completion. Particles so-produced were uniform spheres $\approx$ 15 μm in diameter. However, any predetermined size of such spheres can be easily produced, from a fraction of 1 μm to well over 100 μm.

The above mixtures (binder–solvent–solid pore former) were sonicated to disperse the solids in the liquid, put in syringes, and conducted to the aerosol generator. The mixtures were continuously stirred by magnetic stirrers inside the syringes to ensure uniformity of the dispersion. Aerosols of liquid droplets were, thus, generated inside the thermal reactor. Inert gas (N_2) was flown to disperse and dilute the aerosol, as well as to prevent oxidation. Subsequent evaporation of the solvent produced solid particles. For the case of the PFA, which is a thermosetting polymer, limited secondary polymerization (curing)[42] also took place. Wall temperatures were 240–300°C at the top and 260–360°C at the bottom stages of the reactor for the PFA formulations. Lower temperatures were needed for the PVAC mixtures 190°C top and 230°C bottom. Total residence times of the droplets–particles in the reactor were estimated to be 5–10 s, depending on the size.[41] Residence times were obtained from numerical modeling using the Fluent software.[43] Dry particles were collected at the bottom of the reactor on filters. The PFA-containing particles were subsequently carbonized[42] by heat treatment in a muffler-type furnace, at 600°C, in N_2, for 1 h. Typical volatile loss for PFA was 46%, but particle shrinkage was minimal. The PVAC-containing particles were not carbonized to avert melting and coalescence. All chars were examined by optical and scanning electron microscopy using an OLYMPUS Model VANOX-T and an AMRAY Model 1000 instrument, respectively. BET surface area measurements were conducted in N_2 at 77 K. Mercury porosimetry was conducted using a Micromeritics Autopore II porosimeter capable of achieving a maximum pressure of 4062 atm (60,000 psi).

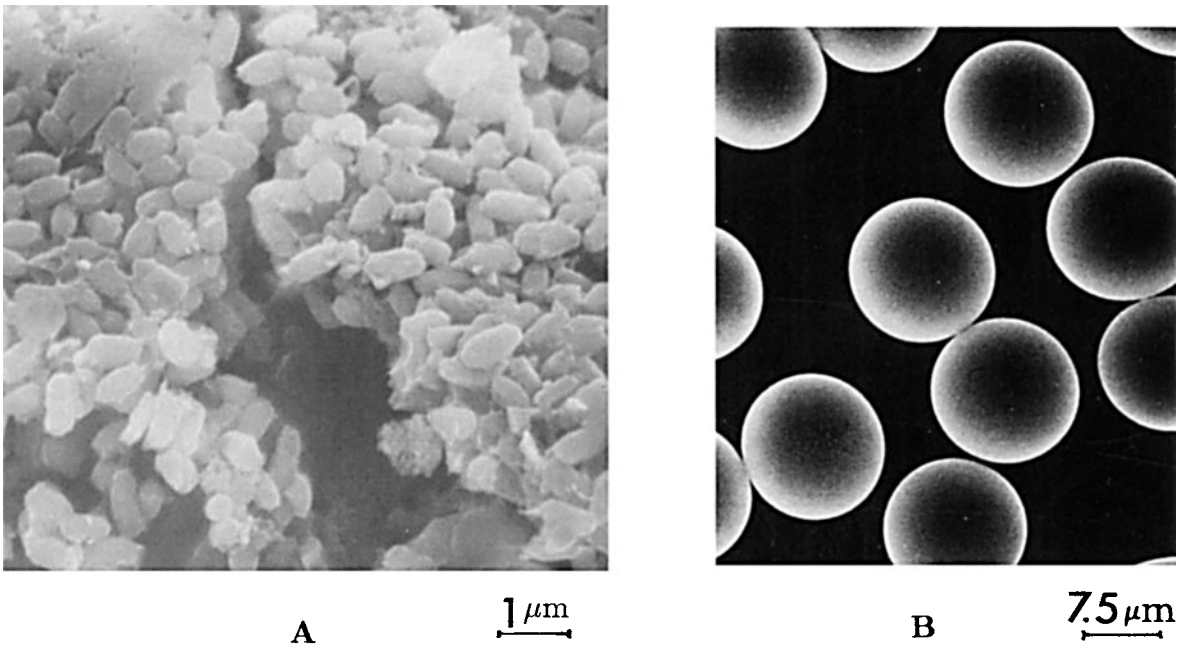

Figure 3 SEM photographs of (a) *Bacillus subtilus* spores and (b) polystyrene spheres.

3. RESULTS AND DISCUSSION

SEM photographs of carbon black aggregates, used as pore formers in the present study, are shown in Figures 2 (a–c). The carbon lamp black and black pearl carbon appear to be similar in structure, with the former having individual spherules $\approx$ 50 nm, and the latter, $\approx$ 100 nm in diameter. The monarch carbon black appears quite different when observed under the SEM. The first two carbon blacks give the impression that the spherules (particles) are stuck together in agglomerates; meanwhile, the monarch black particles appear to be fused together in large entities of matter. *Bacillus subtilus* spores, as detected by SEM, are cylindrical in shape [Fig. 3(a)]. Polystyrene particles are smooth transparent spheres [Fig. 3(b)].

Scanning electron micrographs of the produced PFA particles are shown in Figures 4–9. They have all been carbonized (charred) at 600°C for 1 h. Particles of plain PFA are shown in Figure 4; they appear to be smooth and impermeable, containing no visible porosity. In fact, it has been shown elsewhere that they contain only microporosity.[3,26] These chars were produced in batches of equal-sized particles.

Particles produced from PFA and 20% carbon black (CB) are depicted in Figure 5(a–e) for the three different CBs used in this study. The mass fraction of CB in these PFA–CB particles is more than the 20 wt % put originally in the mixture. This is true because, while the PFA loses mass by releasing volatiles during curing and pyrolysis, the mass of CB remains the same throughout the thermal treatment. Thus, the CB content of these particles can be as high as an estimated 50 wt %. In contrast to the PFA particles that appear to be smooth and impermeable, the PFA–CB particles possess surfaces of various degrees of roughness. It is interesting to notice that although the concentration of the CB filler was the same in all chars the resulting SEM appearance is strikingly different. The carbon lamp black-containing particles appear to be the most porous [Fig. 5(a) and (b)], the black pearl-containing particles appear less rough [Fig. 5(c) and (d)], and, finally, the monarch black-containing particles appear the smoothest [Fig. 5(e)].

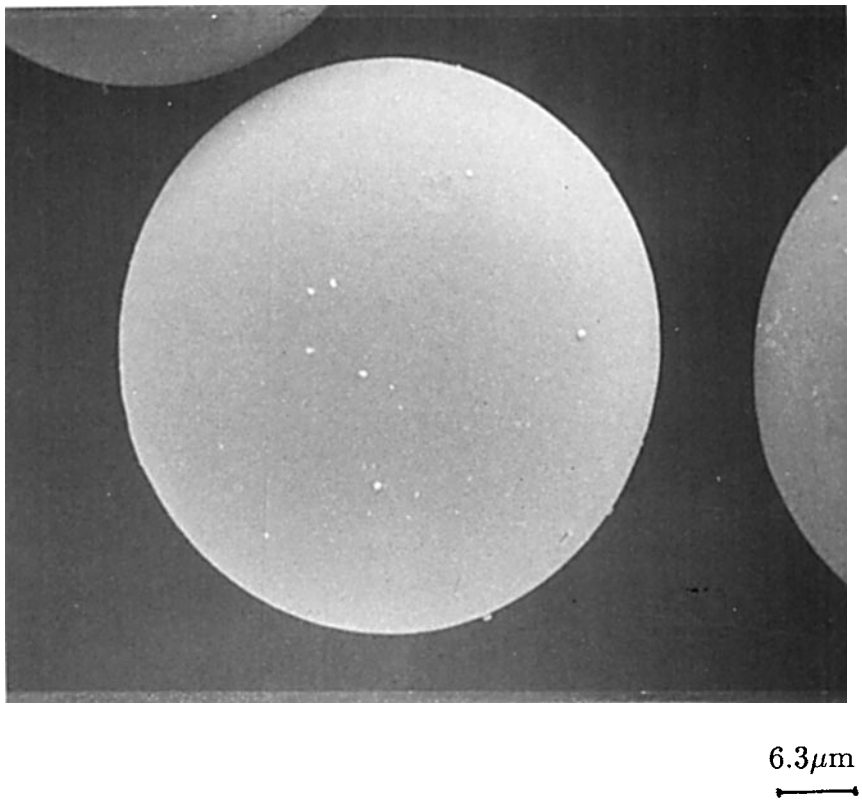

Figure 4 SEM photographs of particles of plain PFA chars.

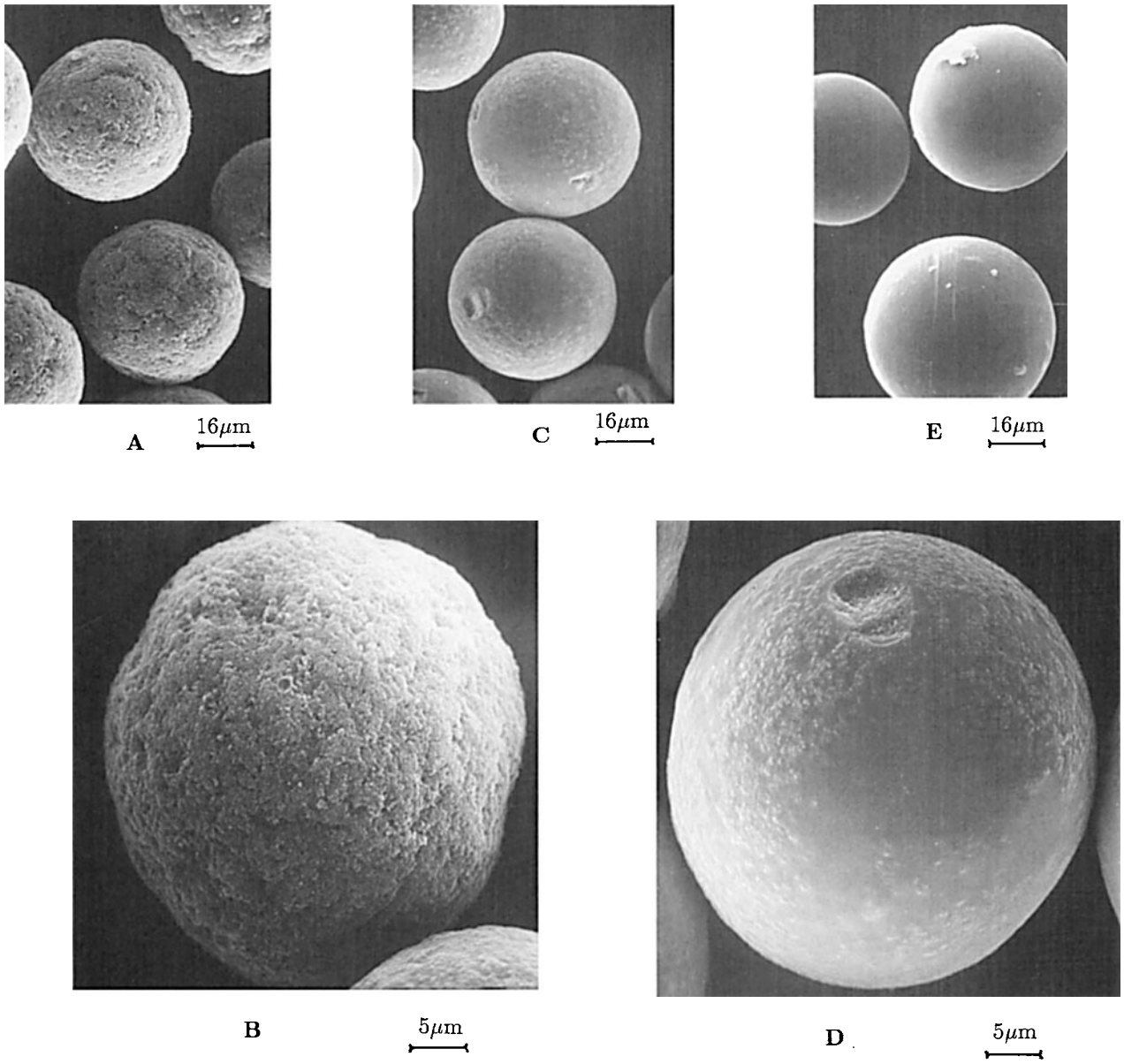

Figure 5 SEM photographs of (a,b) PFA + lamp black; (c,d) PFA + black pearls 120; and (e) PFA + monarch chars.

This phenomenon may be explained on the basis of the different aggregate sizes and structures of these CBs, as was stated earlier [Fig. 2].

BET surface area measurements for all these chars are tabulated in Table I. For the plain PFA particles, the surface area averaged 2 m^2/g, which is similar to the value reported earlier.[26] A surface area of 36 m^2/g was obtained for the case of PFA–CB lamp black chars. For the PFA–CB monarch chars, the BET reading was a surprisingly low: 0.85 m^2/g. The test was repeated again using krypton adsorption, and the same surface area was obtained. For some reason, the monarch carbon black does not seem to promote pore formation, most likely because it does not appear to possess a distinct spherule structure. To the contrary, the chars that contain PFA–CB black pearls have a surface area of 157 m^2/g.

Mercury porosimetry-derived surface areas, densities, and porosities are also given in Table I. Pore volume and surface distributions, as measured by mercury intrusion, for two of the PFA–CB chars are

Table I Physical Properties of Chars

Char	BET Area (m^2)	Mercury Area (m^2)	Bulk Density (g/cm^3)	Mercury Density (g/cm^3)	Porosity (Based on Mercury) (%)
PFA plain	2.9	1.8	1.25	1.33	6
PFA + CB lamp black	34.6	32.7	0.7	1.29	45.7
PFA + CB monarch 1300	0.8	—	—	—	—
PFA + CB black pearl	157	28	1.07	1.4	23.5
PFA + spores	41.5	74.4	0.68	1.33	50
PVAC plain	< 1	—	—	—	—
PVAC + CB lamp black	2.4	—	—	—	—

shown in Figure 6. Pore formation by CB spherules and aggregates may be explained on the basis of stresses developed between the contracting PFA-derived carbon matrix and the CB during pyrolysis and carbonization.[27] As a result of these stresses, cracks develop in the carbon matrix with dimensions of the same order of magnitude as the diameter of the CB spherules.[26,29] Carbon lamp black appears more effective than carbon black pearls in inducing pore formation in the 5–20 nm range (mesopores). The pore-volume distributions of the former chars exhibit a distinct peak at 10 nm and a secondary peak at 30 nm; this same secondary peak is also obvious in the latter chars. The larger black pearl spherules, however, appear to be more successful in creating cracks that render access to the microporous network of the PFA carbon matrix, as evidenced by the higher BET surface-area reading.

Particles prepared from PFA and *Bacillus subtilus* spores are depicted in Figure 7. Since the concentration of the spores in the PFA mixture was again 20% by weight of the PFA and the pores themselves loose volatiles along with the PFA matrix, it was estimated that after pyrolysis and carbonization, the produced chars contain 25–30 wt % of carbonized spores. The produced char particles are brittle, porous, with a few holes, $\approx 0.5\ \mu$ in diameter, scattered on the surface. The BET surface area was 41.5 m^2/g. Pore-volume and surface distributions, deduced from mercury intrusion, are shown in Figure 6. The chars appear highly porous, with a bulk density of 0.68 g/cm^3 containing an enhanced pore network in the region of 5–100 nm, i.e., mesopores to small macropores.

Particles formed from PVAC and PVAC–CB lamp black are shown in Figure 8(a) and (b), respectively. The PVAC particles appeared to be smooth-surfaced, transparent, and colorless, when observed by optical microscopy. No BET surface area was detected for these particles. On the contrary, PVAC–CB particles appeared black in the transmission optical microscope, evident of the high CB content, but in the reflection mode of the optical microscope, as well as the SEM, they appear coated with a smooth polymeric surface. These particles were not pyrolyzed, because when heated at temperatures higher than 300°C, they were observed to deform into a plastic state and melt. Lack of high-temperature treatment is mainly responsible for the small BET surface area.

Chars formed from PFA mixed with poly(styrene) spheres are shown in Figure 9(a) (whole particle) and (b) (fragments). It can be seen from these SEM photographs that the carbon particles contain spherical voids (macropores) of sizes approximately equal to the diameter of the polystyrene spheres. The mechanism of formation of these pores is merely by evaporation of the polystyrene spheres during curing at high temperature. This particular formulation of polystyrene was observed to melt at $\approx$220°C and to vaporize completely at $\approx$400°C. Upon vaporization of the polystyrene, spherical voids were formed. Care was exercised to cure these carbons in steps in order to provide enough time to the PFA carbon matrix to solidify prior to melting of the polystyrene beads. Otherwise, if polystyrene evaporates while PFA is still in a plastic state, any already-formed voids will collapse. Since the polystyrene particles were all of equal size, in this case 15 μm, all macropores are also of approximately equal size. There is no limit to the size of pores that can be produced by this technique. Furthermore, other kinds of pore formers can be used as long as they evaporate to a high degree during the curing step. Poly(methyl methacrylate), poly(vinyl acetate), urea, poly(vinyl butyral), polyterpene, synthetic wax, etc., are candidates for this process. Such particles can be easily produced by the atomization

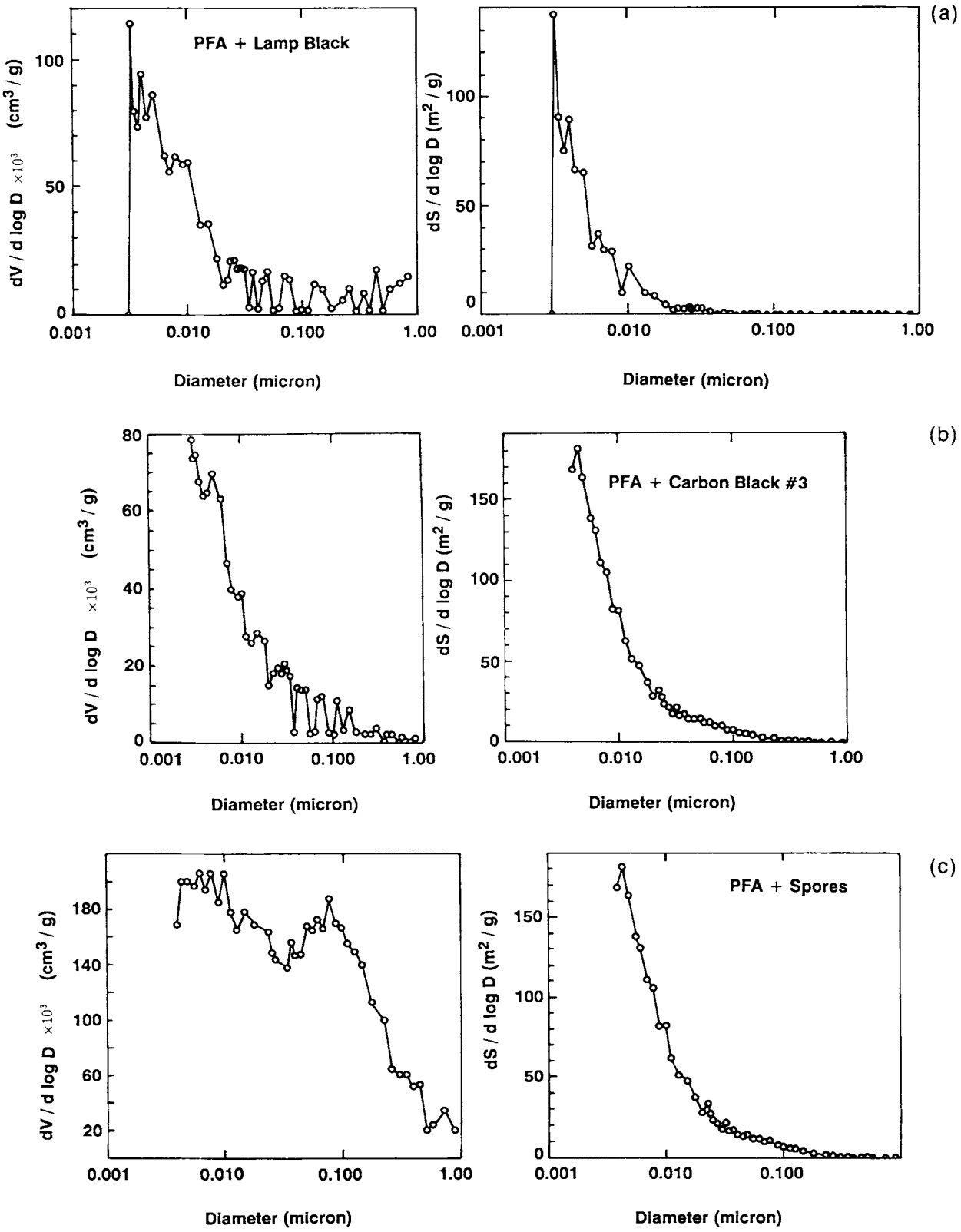

Figure 6 Mercury porosimetry-derived pore volume and area distributions for the following chars: (a) PFA + lamp black; (b) PFA + black pearls 120; (c) PFA + *Bacillus* spores.

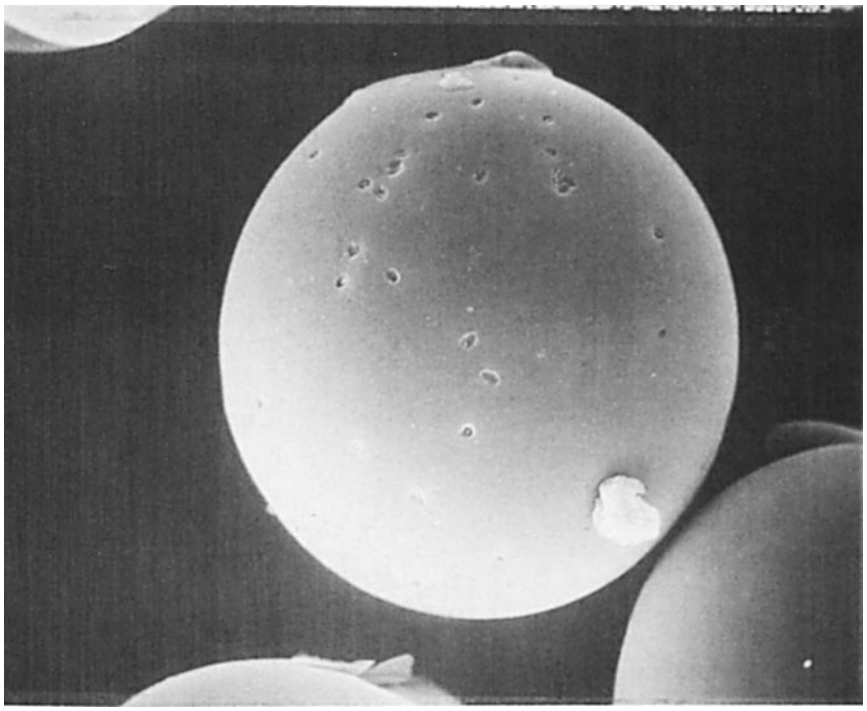

Figure 7 SEM photographs of chars from PFA + *Bacillus subtilus* spores.

technique described herein, in the range of a fraction of 1 μm to a few hundred micrometers. Smaller particles can be made by emulsion polymerization, nucleation of vapors, etc. A previous successful attempt to produce macropores used spores of the licopodium plant.[44] However, such spores always grow to a certain fixed size and they are neither completely spherical nor monodisperse. There are two different kinds of licopodium spores obtained from the *Lycopodium clavatum* and the *Lycopodium alpinum* plants. The former are reticulate spores with a meshed surface structure and a diameter of ≈32 μm, and the latter are rugolose spores with a closed surface structure, ≈ 45 μm in diameter.[45] Furthermore, these spores do not vaporize completely upon carbonization, but instead they leave behind a carbon residue of their own.

4. SUMMARY

Monodisperse batches of spherical, carbonaceous particles have been produced from two polymeric precursors, poly(furfuryl alcohol) (PFA) and poly(vinyl acetate) (PVAC), in a matter of seconds to minutes. Control over the size of the particles was easily achieved by adjusting the parameters of the aerosol generation technique. Control over the porosity and pore structure of the particles was accomplished by using dispersions of solid pore-forming agents, such as different kinds of carbon black (CB) aggregates, bacterial spores, and equal-sized, thermoplastic spheres, like polystyrene. The PFA-derived carbon itself was highly microporous. Use of CB powders, as pore formers, created mesoporosity of various degrees, depending on the physical structure of the aggregates and the dimensions of the individual spherules. Use of bacteria spores enabled formation of meso- and macropores. The most effective and controlled technique, however, to create macropores proved to be the dispersion of thermoplastic spheres throughout the matrix of the thermoset PFA carbon. Such macropores can be generated spherical and monodisperse of a predetermined size. A limited number of runs were conducted herein, to produce PVAC particles. These

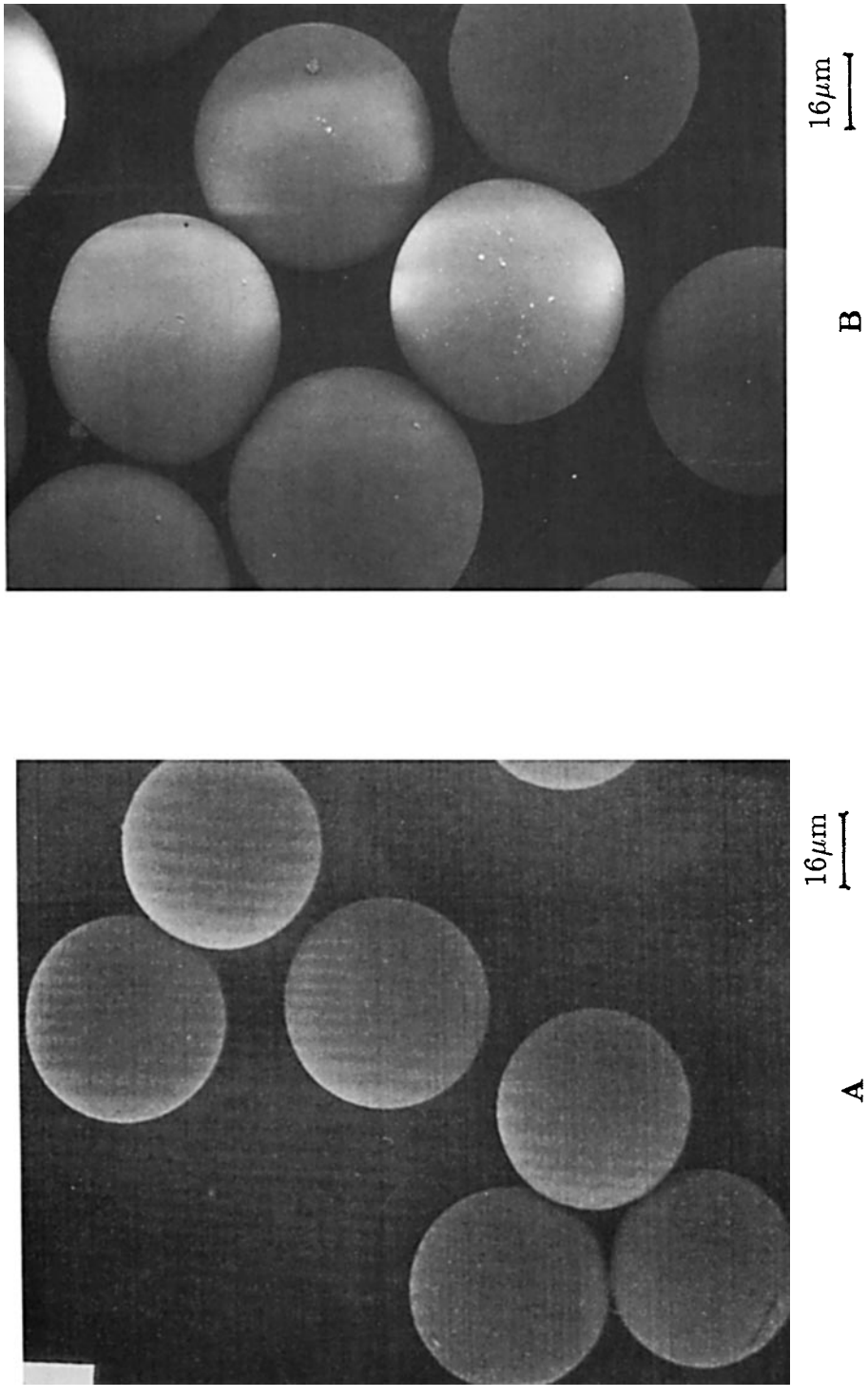

Figure 8 SEM photographs of (a) PVAC particles and (b) PVAC + lamp black particles.

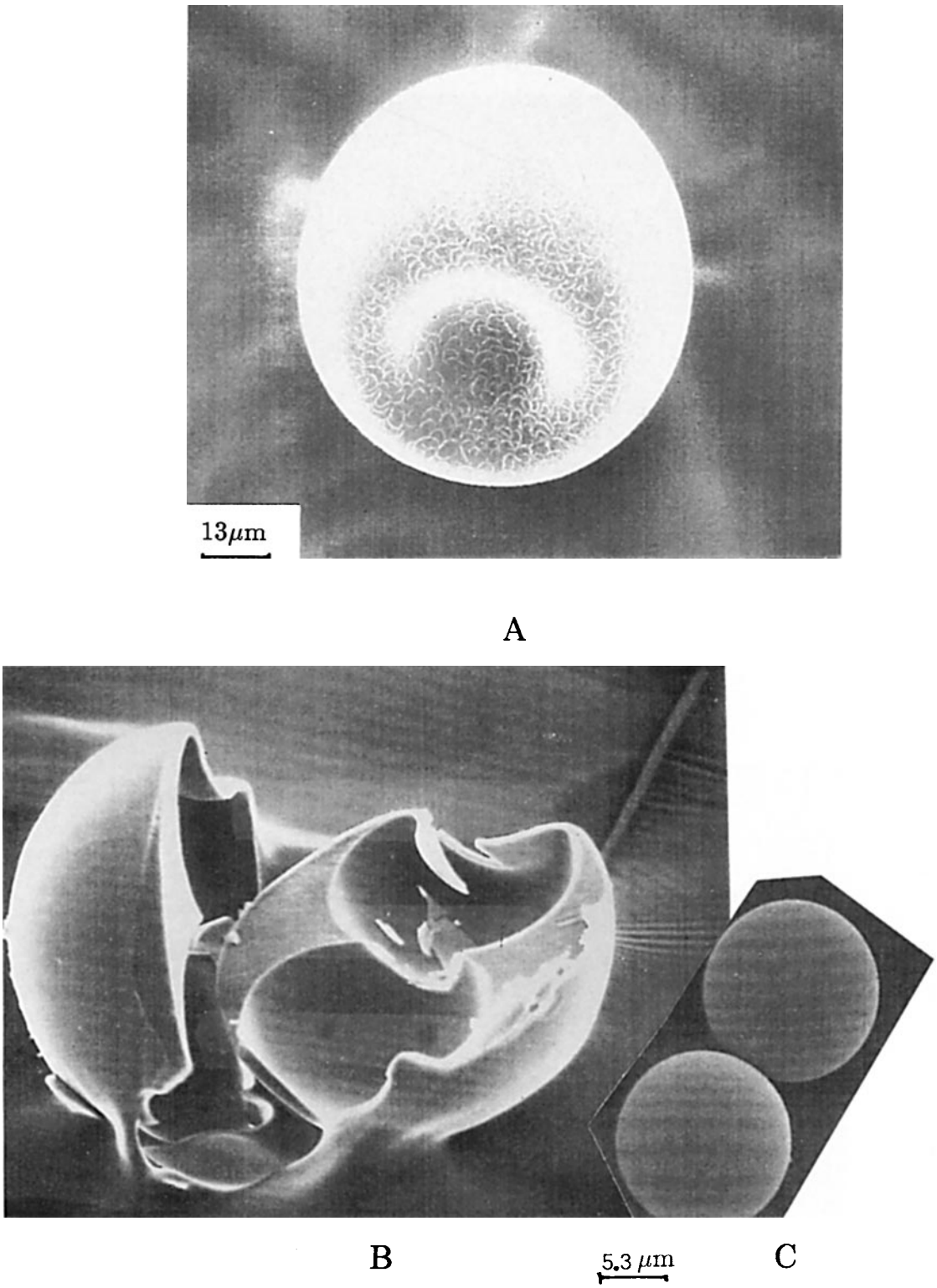

Figure 9 SEM photographs of char particles of (a) PFA + polystyrene and (b) a fragment with spherical voids that were created polystyrene spheres such as those shown in (c).

particles were not thermally treated to avoid melting and deformation. Carbonization of such particles in flight inside a drop tube reactor, however, may afford retention of their sphericity. Such experiments will be conducted in a future investigation.

The authors acknowledge assistance from Mr. Bill Fowle for SEM photography, Dr. Shin-Gyoo Kang for providing the spores and running the mercury porosimetry experiments, and Ms. T. Panagiotou for help with the production of polystyrene spheres. The authors are also indebted to Ms. Marina Belopolsky for help during the char production experiments.

REFERENCES

1. P. J. M. Carrott, R. A. Roberts, and K. S. W. Sing, *Carbon,* **25,** 59 (1987).
2. J. Laine, A. Calafat, and M. Labady, *Carbon,* **7,** 191 (1989).
3. G. M. Jenkins, K. Kawamura, and L. L. Ban, *Proc. R. Soc.,* **A327,** 501 (1972).
4. D. J. Johnson, *J. Phys. D. Appl. Phys.,* **20,** 286 (1987).
5. A. Oberlin, M. Villey, and A. Combaz, *Carbon,* **18,** 347 (1980).
6. G. Porod, *Small Angle X-Ray Scattering,* H. Brumberger, Ed., Gordon & Beach, New York, 1969.
7. J. R. Fryer, *Carbon,* **19,** 431 (1981).
8. D. B. Fishbach and M. E. Rorabaugh, *Carbon,* **21,** 429 (1983).
9. K. S. W. Sing, D. H. Everett, R. A. W. Haul, and L. Meinewska, *Pure Appl. Chem.,* **57,** 603 (1985).
10. H. P. Boehm and M. Voll, *Carbon,* **7,** 227 (1970).
11. P. L. Walker, Jr. and I. Geller, *Nature,* **178,** 1001 (1956).
12. S. P. Nandi, V. Ramadass, and P. L. Walker, Jr., *Carbon,* **2,** 199 (1964).
13. P. S. Northrop, PhD Thesis, Caltech, 1988.
14. R. Sahu, P. S. Northrop, R. C. Flagan, and G. R. Gavalas, *Combust. Sci. Tech.* **60,** 215 (1988).
15. I. Fernandez-Morales, A. Guerrero-Ruiz, F. J. Lopez-Garzon, I. Rodriguez-Ramos, and C. Moreno-Castilla, *Carbon,* **22,** 3, 301 (1984).
16. Y. Toda, N. Yuki, and S. Toyoda, *Carbon,* **10,** 13 (1972).
17. T. G. Lamond, J. E. Metcalfe III, and P. L. Walker, Jr., *Carbon* **3,** 59 (1959).
18. P. L. Walker, Jr., A. Oya, and O. P. Mahajan, *Carbon,* **18,** 378 (1980).
19. K. J. Masters and B. McEnaney, *Abstracts 14th Biennial Conference on Carbon,* 1979, p. 16; B. McEnaney and M. A. Willis, in *High Temperature Chemistry of Inorganic Ceramic Material,* 1977, p. 102.
20. M. M. Dubinin, in *Proceedings 5th Carbon Conference,* Pergamon Press, Oxford, Vol. 1, 1962, p. 81.
21. H. Marsh and W. F. K. Wynne-Jones, *Carbon,* **1,** 269 (1964).
22. E. E. Hucke, U.S. Pat. 3,859,421 (1975).
23. C. Moreno-Castilla, O. P. Mahajian, and P. L. Walker, Jr., *Carbon,* **18,** 271 (1980).
24. E. Fitzer, W. Schaefer, and S. Yamada, *Carbon,* **7,** 643 (1969).
25. E. Fitzer and W. Schäfer, *Carbon,* **8,** 353 (1970).
26. Y. A. Levendis and R. C. Flagan, *Carbon,* **27,** 26 (1989).
27. J. L. Schmitt, Jr. and P. L. Walker, *Carbon,* **9,** 791 (1971); J. L. Schmitt, Jr. and P. L. Walker, *Carbon,* **10,** 87 (1972).
28. C. Moreno-Castilla, O. P. Mahajian, P. L. Walker, Jr., H.-J. Jung, and M. A. Vannice, *Carbon,* **18,** 271 (1980).
29. J. L. Schmitt, Jr., P. L. Walker, Jr., and G. A. Castellion, U.S. Pat. 3,978,000 (1976).
30. G. J. Howard and S. Hutton, *J. Appl. Polym. Sci.,* **19,** 683 (1975).
31. P. Pendleton, B. Vincent, and M. L. Hair, *J. Colloid Interface Sci.,* **80,** 512 (1981).
32. D. H. Everett and F. Rojas, *Chem. Soc. Faraday Trans. 1,* **84**(5), 1455 (1988).
33. S. Gangolli, R. E. Partch, and E. Matijević, *J. Colloid Surf.,* **41,** 339 (1989).
34. B. J. Waters, R. G. Squires, and N. M. Laurendeau, *Combust. Sci. Tech.,* **62,** 187 (1988).
35. C. L. Senior and R. C. Flagan, in *Twentieth Symposium (International) on Combustion,* The Combustion Institute, Pittsburgh, PA, 1986, p. 921.
36. Y. A. Levendis, R. C. Flagan, and G. R. Gavalas. *Combustion Flame,* **76,** 221 (1989).
37. M. Loewenberg and Y. A. Levendis, *Combustion Flame,* **84,** 47 (1991).
38. R. N. Berglund and B. Y. H. Liu, *Environ. Sci. Tech.,* **7,** 147 (1973).
39. N. Sonobe, T. Kyotani, and A. Tomita, *Carbon,* **28,** 483 (1990).
40. K. Daer, Masters Thesis, Northeastern University, 1991.
41. T. Panagiotou and Y. A. Levendis, to appear.
42. H. Eckert, Y. A. Levendis, and R. C. Flagan, *J. Phys. Chem.,* **92,** 5011 (1988).
43. Fluent software by Creare, 1980.
44. S. Niksa, personal communication.
45. G. O. Thomas, G. Oakley, and J. Brenton, *Combustion Flame,* **85,** 526 (1991).

Received September 9, 1991
Accepted October 29, 1991